Femtosecond Spectroscopic Signatures of Electronic Correlations in Conjugated Polyenes and Semiconductor Nanostructures

T. Meier and S. Mukamel

Department of Chemistry and Rochester Theory Center for Optical Science and Engineering, University of Rochester, Rochester, New York 14627

(Received 25 March 1996)

Electronic correlation effects which can be directly probed by ultrafast four-wave mixing are predicted using the electronic-oscillator representation of conjugated polyenes. Comparison with inorganic semiconductors is made possible since the semiconductor Bloch equations projected onto the lowest exciton are obtained as a limiting case. A sign difference in a nonlinear scattering potential clearly shows up in the Wigner spectrogram representing the time and frequency resolved signal. [S0031-9007(96)01433-0]

PACS numbers: 78.66.Qn, 42.50.Md, 71.35.Cc

The calculation of electronic excitations in conjugated polyenes constitutes a complex many-body problem due to the strong correlation effects expected for one-dimensional electronically delocalized systems. *Ab initio* quantum chemistry methods are limited to small systems [1,2]. One important consequence of electronic correlations is the reversal of the positions of the first excited $1B_u$ and $2A_g$ states [1–3]. This shows up in two-photon resonances and affects the fluorescence quantum yield. In this Letter we demonstrate how ultrafast resonant four-wave mixing (FWM) can be used to provide some alternative, dynamical, signatures of electronic correlations in conjugated polyenes. We further compare these with many-body effects observed in inorganic semiconductor nanostructures [4,5]. Our analysis is based on a collective electronic-oscillator description for the response of many electron systems [6], which provides an intuitive picture for the optical response.

We start with the Pariser-Parr-Pople (PPP) Hamiltonian [7], which is known to capture the essential electronic properties of the π electron system [1,8,9].

$$H = \sum_{n,m,\sigma} t_{mn}\hat{c}^{\dagger}_{m,\sigma}\hat{c}_{n,\sigma} + \sum_{n} U\hat{c}^{\dagger}_{n,\uparrow}\hat{c}_{n,\uparrow}\hat{c}^{\dagger}_{n,\downarrow}\hat{c}_{n,\downarrow} + \frac{1}{2}U\sum_{n,m,\sigma,\sigma'}^{n\neq m} \nu_{nm}\hat{c}^{\dagger}_{n,\sigma}\hat{c}_{n,\sigma}\hat{c}^{\dagger}_{m,\sigma'}\hat{c}_{m,\sigma'} - eE(t)\sum_{n,\sigma} z(n)\hat{c}^{\dagger}_{n,\sigma}\hat{c}_{n,\sigma}\,. \quad (1)$$

Here $\hat{c}^{\dagger}_{m,\sigma}$ ($\hat{c}_{n,\sigma}$) is a creation (annihilation) operator for an electron with spin σ at site m (n). The first term is the tight-binding Hückel Hamiltonian, where t_{mn} is the transfer matrix. The Coulomb interaction is given by the next two terms, U is the on-site (Hubbard) repulsion and $\nu_{nm} = [1 + (r_{nm}/a_0)^2]^{-1/2}$ is given by the Ohno formula, with $a_0 = 1.2935$ Å, where r_{nm} is the distance between the nth and mth site. Within the dipole approximation the coupling to an external field polarized along the chain axis is given by $-E(t)\hat{P}$, which is the last term of the Hamiltonian; here e is the electron charge and $z(n)$ is the z coordinate of the nth atom along the chain.

We consider a self-diffraction FWM experiment where the system is excited by two laser pulses with wave vectors $\mathbf{k}_1$ and $\mathbf{k}_2$, and the diffracted signal is monitored in the direction $\mathbf{k}_S = 2\mathbf{k}_2 - \mathbf{k}_1$. We investigate this signal for excitation of the lowest resonance. Using the time-dependent Hartree-Fock (TDHF) scheme, we follow the time evolution of the reduced single-electron density matrix $\rho^{\sigma}_{nm} = \langle\hat{c}^{\dagger}_{m\sigma}\hat{c}_{n\sigma}\rangle$ [9] by solving a closed set of nonlinear equations. The nonlinear polarization that generates the FWM signal is given by $P_S(t) = -e\sum_l z(l)\rho_{ll}(\mathbf{k}_S, t)$. Within the TDHF, the nonlinear optical response of many-electron systems can be exactly mapped onto a coupled set of collective classical oscillators, representing the electron-hole pair component of the single-electron density matrix. This oscillator representation has been used to establish a dominant mode picture for the off-resonant response of conjugated polyenes. Since the spacing between the oscillator frequencies in polyenes is large compared to the spectral width of even very short laser pulses, very few oscillators will contribute resonantly to the present $\chi^{(3)}$ signal. Our numerical calculations are done in real space and include all oscillators. For the interpretation of our numerical results, where we resonantly excite the $1B_u$ oscillator, we found it sufficient to explicitly consider only two oscillators, the lowest B_u oscillator with frequency Ω_1 and one A_g oscillator at $\Omega_2 \approx 2\Omega_1$, representing a two-photon resonance, explicitly. In second order, other A_g oscillators contribute off-resonantly to the response. The effects of these *virtual* oscillators are included via renormalizations of the parameters s_1 and V_1 in Eq. (2). We decompose the equations for the coordinates and the momenta of the oscillators given in Ref. [6] into clockwise and counterclockwise rotating complex parts, and perform a rotating-wave approximation. We then obtain the following equations

for the two oscillators with coordinates p_1 and p_2 ($\hbar = 1$):

$$\partial_t p_1 + \left(i\Omega_1 + \frac{1}{T_2}\right)p_1 = iE(t)(\mu_1 - s_1|p_1|^2) - iV_1|p_1|^2 p_1 + i\mu_{12}E(t)p_2 - iV_{12}p_1^* p_2\,, \quad (2)$$

$$\partial_t p_2 + \left(i\Omega_2 + \frac{1}{T_2'}\right)p_2 = i\mu_{21}E(t)p_1 - iV_{21}p_1^2\,. \quad (3)$$

The polarization is given by

$$P_S(t) = \mu_1 p_1(t) + \mu_{12}p_1^*(t)p_2(t)\,. \quad (4)$$

μ_1 is the dipole moment of oscillator p_1. The nonlinear character of Eqs. (2) and (3) is given by the parameters s_1, V_1, μ_{12}, μ_{21}, V_{12}, and V_{21}, all of which are uniquely determined by the PPP Hamiltonian [6]. s_1 determines the magnitude of the phase space filling, which is the only nonlinearity present in a simple two-level system [10]. The nonlinear potentials V are induced by many-body interactions. By considering a collection of coupled two-level systems within the local-field approximation, one obtains the nonlinear coupling term V_1 [11]. It describes the scattering of oscillator p_1 off itself. Alternatively, in terms of the global eigenstates of the system, this term may be derived from a single three-level system. These two nonlinearities, s_1 and V_1, are included in the semiconductor Bloch equations (SBE) [12,13], extensively used for the description of optical properties in inorganic semiconductors. Recent time-resolved [4] and phase-sensitive experiments [5] have been interpreted using a Ginzburg-Landau-like nonlinear wave equation for the $1s$ exciton amplitude [4,10]. It is equivalent to the ordinary Bloch equations with local-field corrections [10,11]. Formally, this equation can be derived by projecting the SBE on the $1s$ exciton level, neglecting coupling to other states and pure dephasing, i.e., assuming that the population is given by the absolute square of the polarization [5]. The wave equation for the exciton amplitude is a special case of Eq. (2), if the second oscillator p_2 is neglected. Note that, for a linearly driven harmonic three-level system (i.e., equal energy spacing and dipole moments scaling as $\sqrt{2}$), all nonlinear terms cancel identically, and the optical response is purely linear. The PPP Hamiltonian of polyenes requires a multimode extension of Eq. (2). In the present picture we have one additional p_2 oscillator with $\Omega_2 \approx 2\Omega_1$, representing a two-photon resonance at 4.52 eV. μ_{12} and μ_{21} are dipole moments between the two oscillators, while V_{12} and V_{21} are potentials describing their scattering.

The numerical studies shown below compare three models. The first (a) is the Hückel model where electronic correlations are neglected from the outset, $V_1 = V_{12} = V_{21} = 0$. We use the following parameters: $t_{nn} = U\sum_m \nu_{nm}$, $t_{nn+1} = \bar{\beta} - \beta'\Delta z_n$, with $\bar{\beta} = -2.4$ eV, $\beta' = -5.0$ eV Å^{-1}, where Δz_n is the deviation of the bond length from its equilibrium value, and $U = 0$ eV. For the PPP model (c) we use $\beta' = -3.5$ eV, $U = 11.13\ \text{eV}/\epsilon$, with a dielectric constant $\epsilon = 1.5$ [14]. These parameters reproduce the correct band gap of 2 eV for polyacetylene in the long chain limit. However, the effects predicted in this Letter should apply to other conjugated systems as well. For model (c) all coupling terms in Eqs. (2) and (3) are finite. Calculation (b) is an intermediate case, where we use the PPP parameters but neglect the p_2 oscillator and all contributions from virtual oscillators appearing as two-photon resonances. This calculation, in which only a single oscillator is considered explicitly, is performed in order to trace the origin of correlations and to establish a connection with the SBE [12,13].

In the following calculations we investigate a linear 30 carbon atom chain. The two laser pulses have Gaussian envelopes, i.e., $\hat{E}\exp[-(t/\bar{t})^2]$, with $\bar{t} = 20$ fs. We have used phenomenological lifetime-induced dephasing times of $T_2 = 80$ fs and $T_2' = 40$ fs for oscillators p_1 and p_2, respectively. For the observation of the effects discussed below it is required to have laser pulses shorter than the dephasing time.

When the $\mathbf{k}_1$ pulse comes first (positive delay), this technique is known as photon echo. The simplest signature of electronic correlations is the presence of FWM signals for negative time delays (pulse $\mathbf{k}_2$ first), which are absent in a simple two-level system [10,11]. Figure 1 shows the time-integrated FWM signal, $S_{\text{int}}(\tau) = \int_{-\infty}^{\infty}|P_S(t)|^2 dt$, for the three models. In all cases, the signal decays exponentially with the same rate, which is determined by the dephasing time, for positive time delays. For negative delays the signals of models (b) and (c) also decay exponentially with about twice this rate, while the signal (a) is only induced by finite pulse effects and decays much faster, on a time scale determined by the width of the incident pulses (see dash-dotted line in Fig. 1). The time-integrated signal (a) is in agreement with a description based on a simple two-level

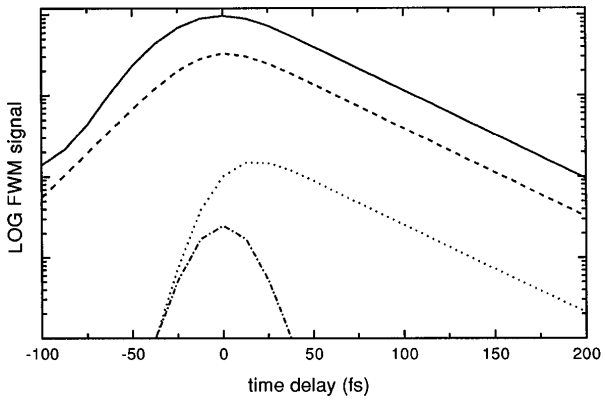

FIG. 1. Time-integrated FWM signals of a 30 carbon atom polyacetylene chain as a function of the time delay for resonant excitation of the lowest resonance at $\Omega_1 = 2.28$ eV; three models are shown (for parameters, see text): (a) Hückel model (dotted), (b) PPP model neglecting two-photon contributions (dashed), (c) full PPP model (solid); also shown is the envelope of the laser pulse (dash-dotted).

system, which, in the ultrashort pulse limit only shows a FWM signal for positive delays [10,11]. For model (a) our calculations show no transition in the vicinity of $2\Omega_1$, and also the contributions from virtual oscillators can be neglected. Therefore the signal is determined by the excitation of just the lowest B_u state. As in a simple two-level system [10,11], the only source of nonlinearity is given by s_1 in Eq. (2), reflecting the phase space filling of the oscillator. The strong signals for negative delays within models (b) and (c) result from electronic correlations.

A more detailed insight on electronic correlation effects is obtained by examining the Wigner spectrogram (WS), which keeps track of both spectral and temporal information contained in an optical signal [15,16].

$$W_S(t,\omega) = \int_{-\infty}^{\infty} P_S^*(t - t'/2) P_S(t + t'/2) e^{i\omega t'} dt'. \quad (5)$$

Upon integrating the WS over time (frequency), we obtain the ordinary frequency-resolved (time-resolved) FWM signals [15]. It can be easily constructed from experiments [5] in which both the amplitude and the phase of the signal are measured. The WS of the FWM signals for our three models are shown in Fig. 2. For model (a) it is completely symmetric with respect to the detuning $(\omega - \Omega_1)$. For short times the signal is spectrally broad, while for longer times only the resonant terms contribute. As a function of time, for zero detuning, it represents a free-induction decay. A two-level model explains very well the temporal and spectral profiles of the WS.

For model (b) the maximum of the WS at zero detuning as a function of time appears to be shifted towards longer times compared to (a); the WS shows an asymmetry with respect to the detuning, with a high frequency (blue) tail. Both of these effects have been observed in inorganic semiconductors. Analytical solutions of the nonlinear wave equation for the $1s$ exciton have shown that it is the scattering of the polarization off itself that explains, in agreement with experimental results, the origin of the delayed time-resolved signal [4,17]. This interaction-induced contribution to the signal has been characterized by a nonlinear scattering potential [4,10], identical to the V_1 term in Eq. (2). The interaction-induced contribution (V_1) is phase shifted by $\pi/2$ with respect to the phase space filling contribution (s_1). The presence of two contributions, with different temporal envelopes, explains the spectral asymmetry of the WS. There is, however, an important difference between inorganic semiconductors and polyenes. While in semiconductors the experimental power spectra are usually asymmetric with a low frequency (red) tail [5], the WS in Fig. 2(b) shows a high frequency tail. Using the expressions for the FWM signal given in Refs. [5] and [10], it can easily be shown that the sign of V_1 determines the direction of the asymmetry of the FWM spectra. Within the SBE, the interaction-induced contribution to the FWM signal is determined by the difference between the field and energy renormalization type many-particle nonlinearities [10,17]. In this language the sign of the potential V_1 implies that, in inorganic semiconductors, usually the field renormalization dominates. In polyenes, if only the $1B_u$ oscillator is considered, V_1 is also positive. The sign change of the effective potential V_1 is induced by virtual A_g oscillators.

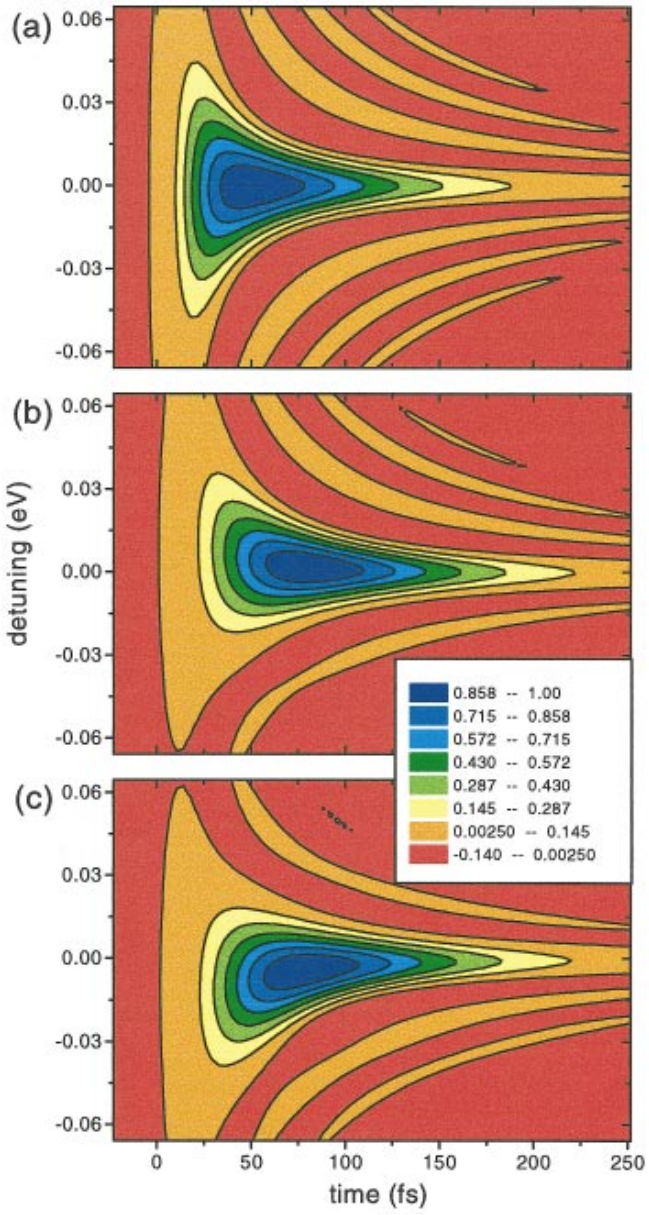

FIG. 2(color). Normalized WS of FWM signals for zero time delay. Shown are models (a), (b), and (c), as indicated (for parameters, see text).

We now discuss the full PPP model (c), i.e. including the second oscillator p_2. The WS has about the same temporal profile as the WS of model (b), but shows a reverse spectral asymmetry, with higher values for negative detuning. Our calculations indicate that the many-body contributions to the FWM signal involving the second oscillator p_2, given by the term V_{12} in Eq. (2), have a different sign than the interaction-induced contributions involving p_1. Additionally, the virtual oscillators representing two-photon resonances change the sign of V_1. Both of these effects result in a phase shift of π of

the interaction-induced contribution to the FWM signal, which, in turn, explains the change of the spectral profile.

In Fig. 3(a) we show the time-resolved amplitude of the FWM signal, which can be obtained from the WS by an integral along the frequency axis [15]. As already pointed out, using the WS, the signal for model (a) has its maximum immediately after the excitation process, while the maxima for the models (b) and (c) are delayed. In all models the time-resolved signals decay exponentially, with a long time rate determined by the dephasing times. In Fig. 3(b) the dynamics of the phase of the FWM signal relative to the phase of the exciting pulses is displayed. Within model (a), such as in a classical driven harmonic oscillator, there is a phase difference of $\pi/2$ between the system response and the exciting force. Formally, it means that the signal, apart from the rotation with $e^{-i\Omega_1 t}$, has a complex prefactor, which can be seen from the term $-iE(t)s_1|P_1|^2$ in Eq. (2). For models (b) and (c) the interaction-induced nonlinearities dominate, leading to a phase difference of about π and 0, respectively. These phase shifts indicate that the interaction-induced signals have a real prefactor. This can be seen by analyzing the V_1 and V_{12} terms in Eq. (2), which have a real prefactor, since the linear p_1 has a purely imaginary prefactor. The difference in sign of the dominant contributions explains why, in model (c), the FWM signal is basically in phase with the exciting laser pulses, while model (b) exhibits a phase shift.

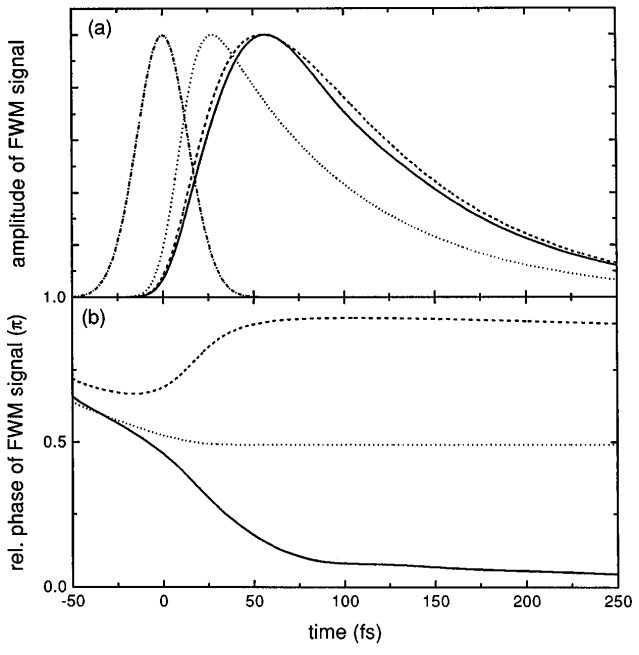

FIG. 3. (a) Normalized time-resolved amplitude and (b) relative phase of the FWM signal for the same models as Fig. 2. The relative amplitudes between the models (a), (b), and (c) are 0.12, 0.55, and 1.0. Models: dotted (a), dashed (b), solid (c); also shown is the envelope of the laser pulse (dash-dotted).

In summary, our analysis shows how amplitude and phase measurements of FWM signals, as displayed in the WS, can be used to measure electronic correlation effects in conjugated polyenes and inorganic semiconductors. The electronic-oscillator representation allows the interpretation of optical nonlinearities in terms of nonlinear scattering potentials and provides a unified description of both types of materials.

We wish to thank Dr. V. Chernyak for discussions and useful comments. The support of the Air Force Office of Scientific Research and the NSF through Grants No. CHE-9526125 and No. PHY94-15583 is gratefully acknowledged. T.M. acknowledges financial support by a fellowship from the scientific branch of NATO through the Deutscher Akademischer Austauschdienst (DAAD).

[1] Z. G. Soos *et al.*, Phys. Rev. B **47**, 1742 (1993).
[2] J. F. Heflin *et al.*, Phys. Rev. B **38**, 1573 (1988); D. C. Rodenberger and A. F. Garito, Nature (London) **359**, 309 (1992).
[3] W. J. Buma, B. E. Kohler, and T. A. Schuler, J. Chem. Phys. **96**, 399 (1992).
[4] S. Weiss *et al.*, Phys. Rev. Lett. **69**, 2685 (1992).
[5] J.-Y. Bigot *et al.*, Phys. Rev. Lett. **70**, 3307 (1993); D. S. Chemla, *et al.*, Phys. Rev. B **50**, 8439 (1994).
[6] V. Chernyak and S. Mukamel, J. Chem. Phys. **104**, 444 (1996).
[7] H. Fukutome, J. Mol. Struct. **188**, 377 (1989), and references therein.
[8] S. Etemad and Z. G. Soos, in *Spectroscopy of Advanced Materials*, edited by R. J. H. Clark and R. E. Hester (Wiley, New York, 1991), p. 87.
[9] A. Takahashi and S. Mukamel, J. Chem. Phys. **100**, 2366 (1994); S. Mukamel *et al.* Science **166**, 251 (1994).
[10] M. Wegener *et al.*, Phys. Rev. A **42**, 5675 (1990).
[11] S. Mukamel, Z. Deng, and J. Grad, J. Opt. Soc. Am. B **5**, 804 (1988); J. Knoester and S. Mukamel, Phys. Rev. A **39**, 1899 (1989).
[12] W. Huhn and A. Stahl, Phys. Status Solidi (b) **124**, 167 (1984); S. Schmitt-Rink, D. S. Chemla, and H. Haug, Phys. Rev. B **37**, 941 (1988); M. Lindberg and S. W. Koch, Phys. Rev. B **38**, 3342 (1988).
[13] H. Haug and S. W. Koch, *Quantum Theory of the Optical and Electronic Properties of Semiconductors* (World Scientific, Singapore, 1994), 3rd ed.
[14] For the calculation of the geometry optimized Hartree-Fock ground state, which enters into the Hamiltonian by a term $\frac{1}{2}\sum_n K(x_n - \bar{x})^2$, where x_n is the nth bond length, we have used a force constant of $K = 21$ eV Å ($K = 38$ eV Å) for the Hückel (PPP) model and an equilibrium bond length of $\bar{x} = 1.41$ Å for both models, see Ref. [9].
[15] L. Cohen, Proc. IEEE **77**, 941 (1989).
[16] R. Trebino and D. J. Kane, J. Opt. Soc. Am. A **10**, 1101 (1993).
[17] M. Lindberg, R. Binder, and S. W. Koch, Phys. Rev. A **45**, 1865 (1992).